

## 2 THE ELECTRON-ION COLLIDER (EIC)

### 2.1 The Electron Ion Collider Science

Elke C. Aschenauer (\*) and Markus Diefenthaler (\*\*)

Mail to: [elke@bnl.gov](mailto:elke@bnl.gov)  
[mdiefent@jlab.gov](mailto:mdiefent@jlab.gov)

(\*) Brookhaven National Laboratory, Upton, NY 11973, USA

(\*\*) Thomas Jefferson National Accelerator Facility, Newport News, Virginia, USA

#### 2.1.1 Introduction

Quantum Chromodynamics (QCD), the theory of the strong interaction, is a cornerstone of the Standard Model of modern physics. It explains all nuclear matter as bound states of point-like fermions, known as quarks, and gauge bosons, known as gluons. The gluons bind not only quarks but also interact with themselves. Unlike with the more familiar atomic and molecular matter, the interactions and structures are inextricably mixed up, and the observed properties of nucleons and nuclei, such as mass and spin, emerge out of this complex system. The mass of the nucleon e.g. is not due to its nearly massless quarks (and massless gluons) but originates from the self-generating gluon field and the quark-gluon interactions. The similarity of mass between the proton and neutron arises from the fact that their internal gluon dynamics are the same. The key aspects of QCD, asymptotic freedom, chiral symmetry breaking, and color confinement, are driven by gluons. Despite the fundamental role of gluons, and the many successes in our understanding of QCD, the properties and dynamics of gluons remain largely unexplored.

To precisely image the quarks and gluons and their interactions and to explore the new QCD frontier of strong color fields in nuclei, the Nuclear Physics community proposes an US-based Electron Ion collider (EIC) with high-energy and high-luminosity, capable of a versatile range of beam energies, polarizations, and ion species. The community is convinced that the EIC is the right tool to understand how matter at its most fundamental level is made. In recognition of this, the Nuclear Science Advisory Committee advising the Department of Energy and the National Science Foundation, recommended in its Long Range Plan in 2015 an EIC as the highest priority for new facility construction [1].

Subsequently, a National Academy of Sciences panel was charged to review both the scientific opportunities enabled by a U.S. based EIC and the benefits to other fields of science and society [2]. The National Academy of Sciences report strongly articulates the merit of an EIC: *“In summary, the committee finds a compelling scientific case for such a facility. The science questions [ How does the mass of the nucleon arise? How does the spin of the nucleon arise? What are the emergent properties of dense systems of gluons?] that an EIC will answer are central to completing an understanding of atoms as well as being integral to the agenda of nuclear physics today. In addition, the*

*development of an EIC would advance accelerator science and technology in nuclear science; it would as well benefit other fields of accelerator-based science and society, from medicine through materials science to elementary particle physics.”*

This positive report could be the basis for a Critical Decision-0 or Mission Need approval for the Department of Energy Office of Science, setting in motion the process towards formal project R&D, engineering and design, and construction. The DOE Office of Nuclear Physics is already supporting increased efforts towards the most critical generic EIC-related accelerator research and design.

### 2.1.2 The Secrets of Nucleons and Nuclei

Deep-inelastic scattering (DIS), the basic process at the EIC, is because of its unmatched precision the ideal tool to study the inner structure of nuclear matter. The distribution of partons insight nucleons and nuclei depends on the scale,  $Q^2$ , which specifies the resolution at which partons are resolved, and the momentum fraction,  $x$ , carried by the parton relative to the momentum of the nucleon. Both variables ( $x, Q^2$ ) define the kinematics and regime probed in a DIS measurement and can be controlled event-by-event. Figure 1 shows schematically how going from high  $x$  ( $\sim 1$ ) to small  $x$  ( $\sim 10^{-4-5}$ ) at a resolution scale  $Q^2$  of a few  $\text{GeV}^2$  reveals a more and more complicated structure of quarks and gluons inside the proton. The proton goes from a few-body regime with its structure dominated by the valence quarks to a many-body regime dominated by the quark-gluons dynamics responsible for hadron structure, to a collective regime dominated by gluons generated through QCD radiation and at last to the saturation regime where the parton densities are so large that the gluon radiation is balanced by gluon recombination leading to non-linear effects.

Understanding the observed properties of nucleons or nuclei, such as mass or spin, requires to be able to probe all regimes and the transition from one regime to the other and to explore how the observed properties emerge from the complex, strongly-interacting many-body systems of nuclear matter. The EIC with versatile beam energies and species and a broad range in  $x$  and  $Q^2$  will be the right tool to unravel the QCD structures and dynamics of matter.

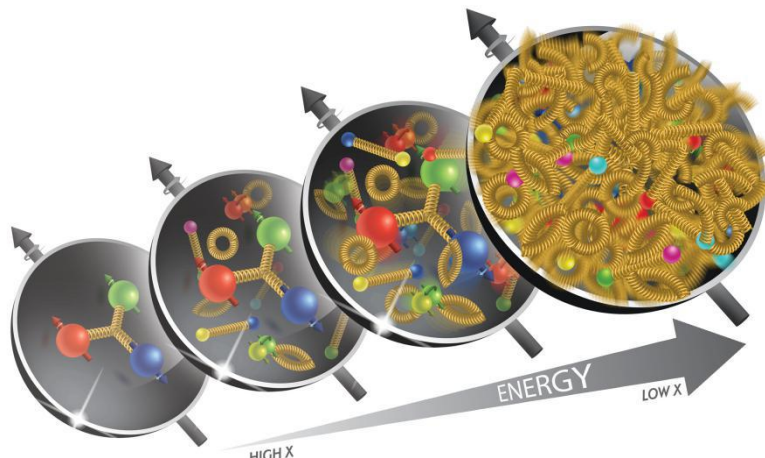


**Figure 1:** The development of the internal quark and gluon structure of the proton going from high to low  $x$ . Decreasing  $x$  corresponds to increasing the center-of-mass energy.

Till today the consolidated understanding of the nucleon structure is basically one-dimensional. In inclusive DIS, the nucleon appears as a bunch of fast-moving quarks, antiquarks and gluons, whose transverse positions and momenta are not resolved. EIC will open up the unique opportunity to go far beyond this one-dimensional picture of the nucleon. It will enable parton femtoscopy by imaging quarks and gluons in transverse position and momentum space for all kinematic regimes. Such “tomographic images” will provide insight into the QCD dynamics inside hadrons, such as the interplay between sea quarks and gluons and the role of pion degrees of freedom at large transverse distances.

Hadron structure cannot be understood without unraveling spin structure. While past or existing DIS experiments were and are very successful in determining the polarized quark structure of the nucleon and of some light nuclei, none matches the unique capabilities of an EIC by being able to change at the same machine between longitudinal, transverse, and (for deuteron only) tensor polarization states and with being able to collide polarized electron beams with polarized protons, deuteron, and Helium-3 beams over a broad kinematic range.

The capability of electron-ion collision with a wide range in  $A$  at the EIC will allow to extend the “tomographic images” to nuclei to gain insight into the short-range structure of nuclei. Nuclei are made out of nucleons, which in turn, are bound states of the fundamental constituents, quarks and gluons, probed in high-energy scattering. The binding of nucleons into a nucleus must be sensitive to how these quarks and gluons are confined into nucleons and must influence how they are distributed inside the bound nucleons. EMC at CERN [3] and many follow-up experiments revealed a peculiar pattern of nuclear modification of the DIS cross-section as a function of Bjorken  $x$ , giving us clear evidence that the momentum distributions of quarks in a fast-moving nucleus are strongly affected by the binding and the nuclear environment. With much wider kinematic reach in both  $x$  and  $Q^2$ , and unprecedented high luminosity, experiments at EIC not only can explore the influence of the binding on the momentum distribution of sea quarks and gluons, but also, study how quark-gluon interactions create nuclear binding.

Both nucleons and nuclei, when viewed at high energies, appear as dense systems of gluons creating fields whose intensity may be the strongest in nature. These high densities will possibly lead to the phenomenon of parton (gluon) saturation [4,5]. The transition from the collective to saturation regime is characterized by the saturation momentum,  $Q_S$ , which can be large for heavy ions. By studying the collisions of high energy nuclei with energetic electrons, one might be able to probe the strong gluon fields beyond the collective regime as suggested by HERA, RHIC, and the LHC data and identify the saturation regime and its parameters.

The unique kinematic reach of the EIC for polarized electron-proton and electron-ion collisions is illustrated in Figure 2.

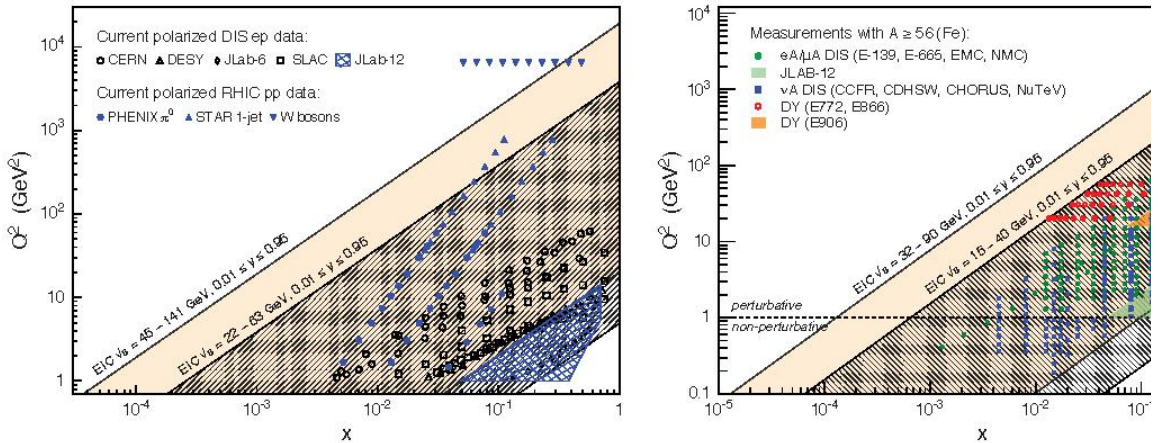


**Figure 2:** *Left:* The range in parton momentum fraction  $x$  vs. the square of the momentum transferred by the electron to the proton  $Q^2$  accessible with EIC in polarized ep collisions for two different center-of-mass regions ( **$\sqrt{s} = 22 - 63$  GeV and  $45 - 141$  GeV**) compared to past (CERN, DESY, SLAC) and existing (JLAB, COMPASS) facilities as well to polarized pp collisions at RHIC. *Right:* The kinematic acceptance in  $x$  and  $Q^2$  of completed lepton-nucleus (DIS) and Drell-Yan (DY) experiments (all fixed target) compared to the EIC acceptance for two different center-of-mass regions ( **$\sqrt{s} = 15 - 40$  GeV and  $32 - 90$  GeV**). The acceptance bands for EIC are defined by  $Q^2 = xsy$  with  **$0.01 \leq y \leq 0.95$** .

### 2.1.3 The Spin of the Nucleon

Helicity-dependent parton densities encode the information to what extent quarks and gluons with a given momentum fraction  $x$  tend to have their spins (anti-)aligned with the spin direction of a nucleon. The most precise knowledge about these non-perturbative quantities, along with estimates of their uncertainties, is gathered from comprehensive global QCD analyses [6,7] to all available data taken in spin-dependent DIS and proton-proton collisions, with and without additional identified hadrons in the final state.

Apart from being essential for a comprehensive understanding of the partonic structure of hadronic matter, helicity PDFs draw much their relevance from their relation to one of the most fundamental and basic but yet not satisfactorily answered questions in hadronic physics, namely how the spin of a nucleon is composed of the spins and orbital angular momenta of quarks and gluons. The integrals of helicity PDFs over all momentum fractions  $x$  (first moments) at a resolution scale  $Q^2$ ,  $\Delta f(Q^2) \equiv \int_0^1 \Delta f(x, Q^2) dx$ , provide information about the contribution of a given parton flavor  $f$  to the spin of the nucleon. A precise determination of the polarized quark  $\Delta q(x, Q^2)$  and gluon  $\Delta g(x, Q^2)$  distribution functions in a broad kinematic regime is a primary goal of the EIC.

Several channels are sensitive to  $\Delta g$  in ep scattering at collider energies such as DIS jet or charm production, but QCD scaling violations in inclusive polarized DIS have been identified as the golden measurement. Scaling violations are a key prediction of QCD

for PDFs and have been used successfully at HERA to determine the unpolarized gluon distribution with high precision. The inclusive DIS structure function  $g_1(x, Q^2)$  is the most straightforward probe in spin physics and has been determined at various fixed-target experiments at medium-to-large values of  $x$  in the last two decades. It is also the best-understood spin-dependent quantity from a theoretical point of view.

For studying DIS scaling violations, i.e.,  $dg_1(x, Q^2)/d\log Q^2$ , efficiently, it is not only essential to have good precision but also to cover the largest possible range in  $Q^2$  for any given fixed value of  $x$ . The accessible range in  $Q^2$  is again linked to the capabilities of detecting electrons in an as wide as possible range of momenta and scattering angles. Figure 3 (left) illustrates the simulated data sets for inclusive polarized DIS at the EIC for three different choices of center of mass energies. The error bars reflect the expected statistical accuracy for an integrated luminosity of  $10 \text{ fb}^{-1}$  and assuming 70% beam polarizations. The uncertainties of the DSSV14 theoretical prediction [7] are shown by the blue bands.

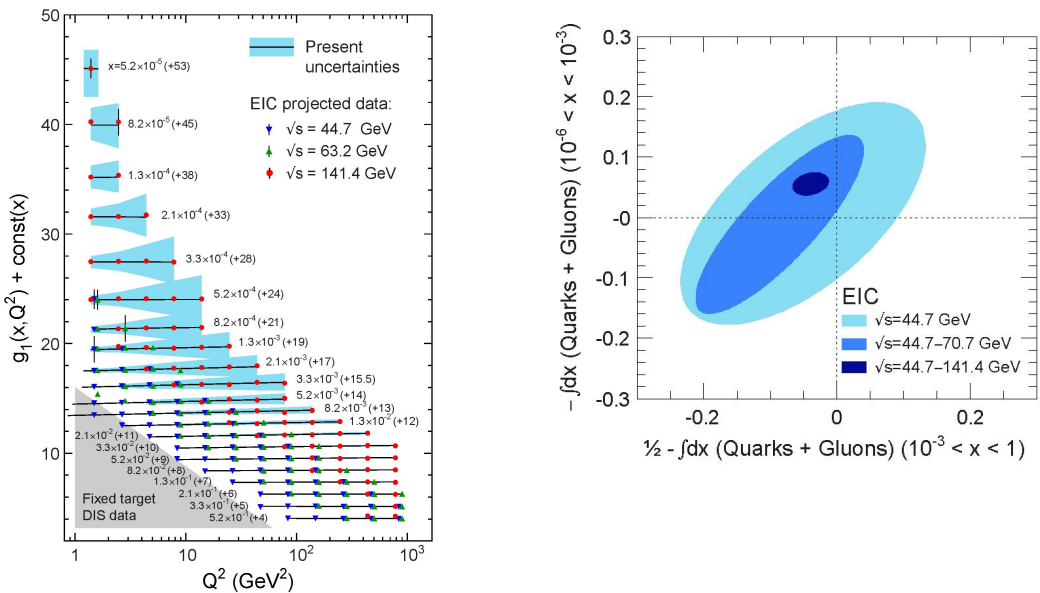


**Figure 3:** *Left:* Projections for the structure function  $g_1(x, Q^2)$  at different center of mass energies, compared with a model extrapolation and its uncertainties [8]. The curves correspond to different values of  $x$  that are specified next to each curve. For clarity, constants are added to  $g_1$  to separate different  $x$  bins; moreover, multiple data points in the same  $x$ - $Q^2$  bin are displaced horizontally. The gray area marks the phase space currently covered by fixed target experiments.

*Right:* The EIC's impact on the knowledge of the integral of the quark and gluon spin contribution in the range  $10^{-6} < x < 10^{-3}$  (y-axis) versus the contribution from the orbital angular momentum in the range  $10^{-3} < x < 1$  (x-axis).

Figure 3 uses simulated data to clearly demonstrate the EIC's impact on the knowledge of the integral of the proton's quark and gluon spin contributions for  $10^{-6} < x < 10^{-3}$  versus the contribution to the orbital angular momentum for the range  $10^{-3} < x < 1$ . A dramatic shrinkage of the uncertainties in the parton helicities is seen with the largest energy reach. The underlying reason for this rapid shrinkage can be traced to the completely unknown behavior of  $g_1(x, Q^2)$  due to the lack of data at small  $x$ .

The full understanding of the flavor separated of the spin structure of protons and neutrons will require measurements of transverse spin asymmetries to measure the transversity distribution and deuteron and/or Helium-3 beams.

#### **Machine Requirements for Polarized Deep Inelastic Scattering:**

The measurement of spin asymmetries requires longitudinally polarized electrons off longitudinally (or transversely) polarized light hadron beams (proton, Deuterium and/or He-3) with high polarization values ( $> 70\%$ ). Experimental systematic uncertainties, coming from polarization measurements and other (time dependent, detector related) false asymmetries in measurements have to be constrained to a few percent [8]. High energy beams will allow to probe the missing spin contributions of quarks and gluons at  $10x$ .

#### **2.1.4 Nucleons and Nuclei in 3-Dimensions**

From inclusive DIS measurements we can only learn about the longitudinal motion,  $x$ , of partons (see Figure 4) in a fast-moving nucleon but no information about the transverse positions or momenta of partons can be obtained. Even though a fast-moving nucleon is Lorentz-contracted, its transverse size is still about 1 fm, which is the typical scale of non-perturbative interactions, where phenomena such as confinement occur. This leads to fundamental questions such as:

- How are quarks spatially distributed inside the nucleon?
- How do they move in the transverse plane?
- Is there a correlation between orbital motion of quarks, their spin, and the spin of the nucleon?
- How can we access information on such spin-orbit correlations, and what will this tell us about the nucleon?

The above questions address two complementary aspects of the nucleon structure: the distribution of quarks and gluons in the transverse plane in momentum space and in coordinate space. We still lack quantitative answers to these questions, but in recent years we have obtained a much better idea on how to answer them due to recent theoretical progress [8]. Generalized parton Distributions (GPDs) and transverse momentum dependent parton distributions (TMDs) are the novel tools in QCD that allow us to study the inner structure in three dimensions. In addition to the longitudinal momentum fraction  $x$ , GPDs provide information about the transverse position  $b_T$  (see Figure 5). TMDs describe the inner structure in momentum space as a function of  $x$  and the transverse momentum  $k_T$  (see Figure 6). They encode information about spin-orbit correlations in nuclear matter.

To precisely image the momentum and spatial structure of quarks and gluons is one of the key goals of an EIC.

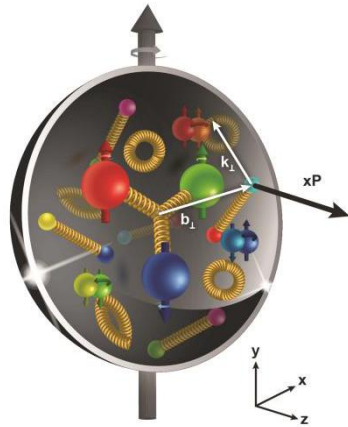


**Figure 4:** Schematic view of a parton inside the proton with longitudinal momentum fraction  $x$ , transverse position  $\mathbf{b}_T$  and transverse momentum  $\mathbf{k}_T$  in the proton.

The EIC will probe TMDs in the few-body, many-body and collective regime. The high luminosity and broad kinematic coverage of the EIC will allow for a high-precision measurement of TMDs for quarks taking all kinematic correlations into account in a multi-dimensional analysis in  $x$ ,  $Q^2$ ,  $\Phi_S$ ,  $p_T$ ,  $z$ , and  $\Phi$ . The kinematic reach of the EIC will provide not only a broad coverage in  $x$ ,  $0.01 < x < 0.9$  and a sufficiently high  $Q^2$  to suppress higher twist contributions but will enable the first measurement of TMDs for sea quarks and the first measurement of TMDs for gluons by tagging the photo-gluon fusion process. The coverage of the few-body, many-body and collective regimes is ideal for systematic studies of TMD evolution and stringent tests of the underlying theory of TMDs.

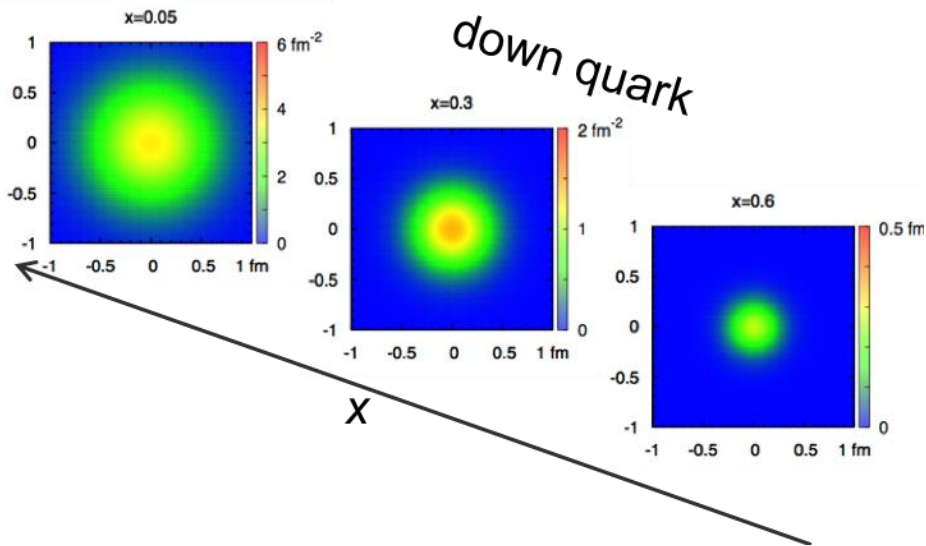


**Figure 5:** Transverse position snapshots of a down quark in an unpolarized nucleon for three values in  $x$ . The color coding of the three panels indicates the probability of finding the down quark.

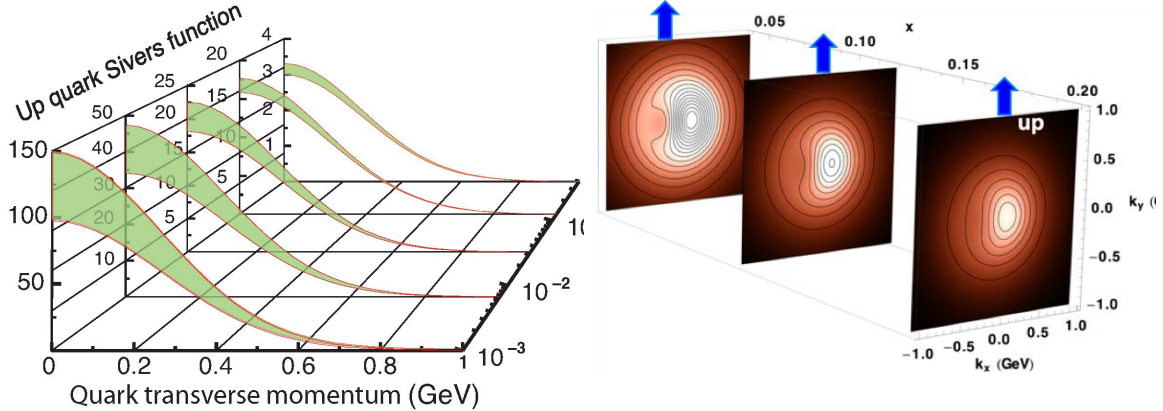


**Figure 6:** *Left:* The transverse momentum profile of the Sivers TMD for up quarks for five  $x$  values accessible at the EIC, and corresponding statistical uncertainties. *Right:* Transverse momentum snapshots of a transversely polarized nucleon (polarization direction indicated in blue) for three values in  $x$ . The color coding of the three panels indicates the probability of finding the up quark.

The EIC will allow to study GPD in various processes in the few-body, many-body and collective regime. The flavor decomposition of GPDs and their dependence on the polarization can be studied for valence and sea quarks in measurements of electro-production of  $\pi^+$ ,  $K^{+/-}$ ,  $\rho$ , and  $K^*$ . Measurements of deeply virtual Compton scattering [9] and the exclusive production of  $J/\Psi$ ,  $\rho$  and  $\varphi$  mesons will allow to constrain transverse position distributions of sea quarks and gluons and their spin-orbit correlations.

An unique opportunity of the EIC is to study GPDs and TMDs in nuclei and learn about their nuclear dependence.

#### Machine Requirements for Nucleons and Nuclei in 3-Dimensions:

Measurements of GPDs and TMDs require longitudinally polarized electrons off longitudinally and transversely polarized light hadron beams (proton, Deuterium and/or He-3) with high polarization values ( $> 70\%$ ). High luminosity ( $10^{33-34} \text{ cm}^{-2}\text{s}^{-1}$ ) is required for a multidimensional analysis taking all the kinematic correlations into account. Versatile beam energies are required to probe the few-body, many-body and collective regime and for a broad coverage in  $Q^2$ .

##### 2.1.5 Physics at high Parton Densities

DIS experiments with nuclei have established that PDFs (or structure functions) in nuclei compared to the ones of a free proton exhibit various nuclear effects, not surprisingly most prominent for gluons: a strong suppression of the gluon distribution function in nuclei compared to that in nucleons for  $x < 0.01$  (shadowing), and slight enhancement around  $x \sim 0.1$  (anti-shadowing), followed again by a suppression (EMC effect [3]) at large  $x$ . In sharp contrast to the proton, the gluonic structure of nuclei is not known for  $x < 0.01$ . Measurements of the inclusive cross section with and without

charm tagging in the final state will considerably constrain these distributions down to  $x = 10^{-4}$ . To emphasize the precision achievable at an EIC, two examples of the reduced cross-section as a function of  $x$  at the  $Q^2$  values of  $4.4 \text{ GeV}^2$  and  $139 \text{ GeV}^2$  are shown in Figure 7 for inclusive (left) and charm (right) production. It is clear from Figure 7 that at large values of  $x$ , the uncertainties are small. It is only at  $x < 10^{-2}$  and small  $Q^2$  that the expected experimental errors on the EIC measurements become much smaller than the uncertainties from the EPPS16 parametrization that are largest at the smallest  $x$  values; these will clearly be significantly constrained by data at these  $x$  values.

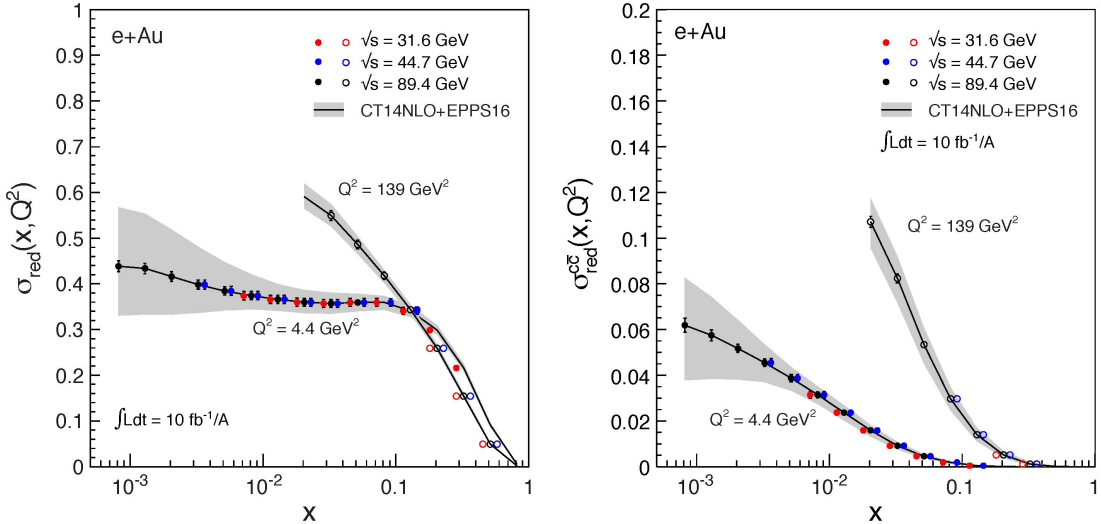


**Figure 7:** Inclusive (left) and charm (right) reduced cross-sections as a function of  $x$  at the  $Q^2$  values of  $4.4 \text{ GeV}^2$  (solid circles) and  $139 \text{ GeV}^2$  (open circles) at three different center-of-mass energies.

The modification introduced by the nuclear environment can be quantified in terms of the ratio between the nucleus  $A$  and the free proton PDF ( $R_f^A$ ,  $f = q, g$ ) for quarks and gluons, with deviations from unity being manifestations of nuclear effects. A depletion of this ratio relative to unity is often called shadowing. The impact study of EIC simulated data shown in Figure 7 was done by incorporating these data into the EPPS16 fit [10]. However, as the parameterization is too stiff in the as yet unexplored low  $x$  region, additional free parameters for the gluons have been added to the functional form (EPPS16\* [11]). The corresponding  $R_g^{Pb}$  from EPPS16\* is shown in Figure 8.

The grey band represents the EPPS16\* theoretical uncertainty. The orange band is the result of including the EIC simulated inclusive reduced cross-section data in the fit. The lower panel of each plot shows the reduction factor in the uncertainty (orange curve) with respect to the baseline fit (gray band). It is clear that the higher center-of-mass energy has a larger impact in the whole kinematical range with the relative uncertainty roughly a factor of 2 smaller than for the lower center-of-mass energy. The blue hatched bands show the simulated charm quark reduced cross-section for which no data currently exist. While it brings no additional constraint on the low- $x$  region, its impact at high- $x$  is remarkable providing up to a factor 8 reduction in uncertainty (blue curve).

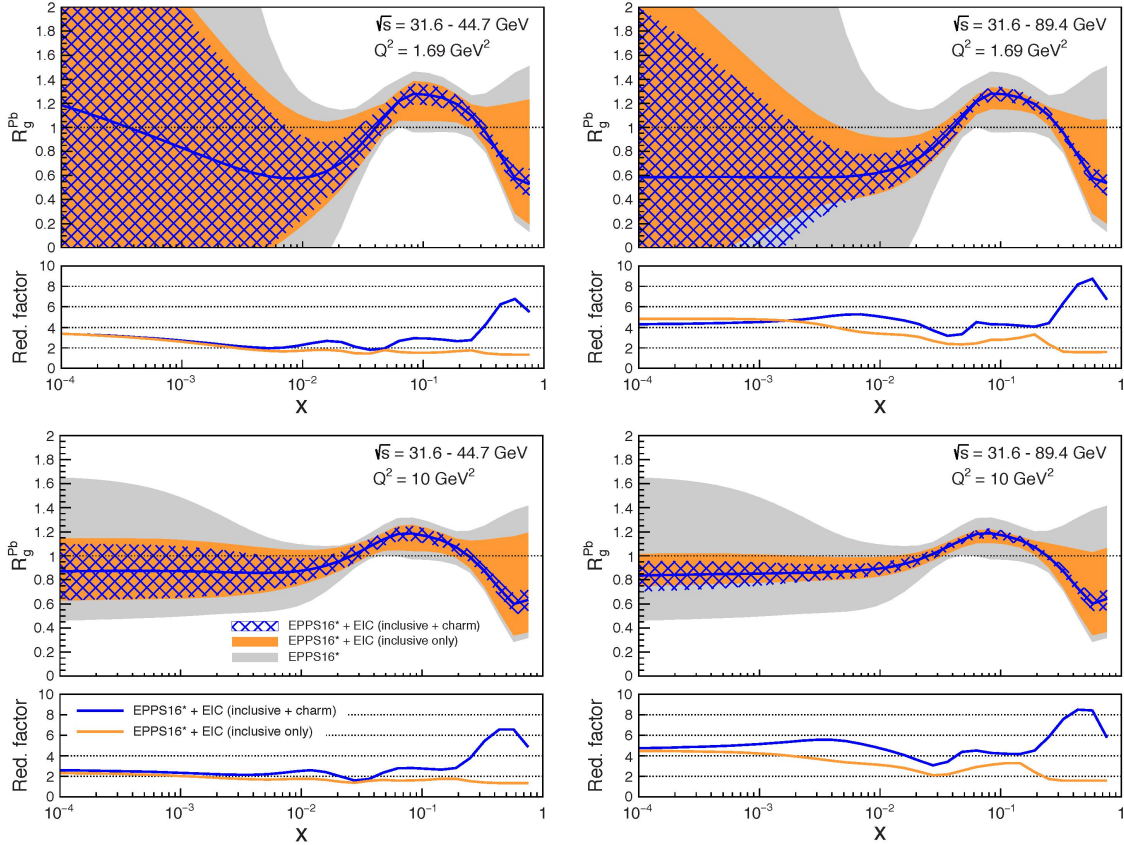


**Figure 8:** The ratio  $R_g^{Pb}$ , from EPPS16\*, of gluon distributions in a lead nucleus relative to the proton, for the low (left) and high (right)  $\sqrt{s}$ , at  $Q^2 = 1.69 \text{ GeV}^2$  and  $Q^2 = 10 \text{ GeV}^2$  (upper and lower plots, respectively). The grey band represents the EPPS16\* theoretical uncertainty. The orange (blue hatched) band includes the EIC simulated inclusive (charm quark) reduced cross-section data. The lower panel in each plot shows the reduction factor in the uncertainty with respect to the baseline fit.

The nucleon is a complex system of strongly interacting quarks and gluons. In addition to the valence quarks dominating the nucleon structure at large values of  $x$ , there is a “sea” of quarks, antiquark, and gluons popping in and out of existence and defining the nucleon structure in the many-body and collective regimes for intermediate and small  $x$ . While the nucleon sea originates from various contributions, it is dominated in the collective regime by gluons radiating off quark-antiquark pairs and other gluons.

However, gluon and quark densities cannot grow without limit at small- $x$ . While there is no strict bound on the number density of gluons in QCD, there is a bound on the scattering cross-sections stemming from unitarity [12]. A nucleon or nucleus with a lot of “sea” gluons is more likely to interact in high-energy scattering, which leads to larger scattering cross-sections. Gluon saturation is a mechanism to tame this growth: When the gluon density becomes large, softer gluons can recombine into harder gluons. The competition between linear QCD radiation and non-linear gluon recombination causes the gluon distributions to saturate at small  $x$ . The onset of saturation and the properties of the saturated phase are characterized by a dynamical scale, the saturation scale [13,14,15],  $Q_s^2$ , which grows with increasing energy (smaller  $x$ ). The saturation regime is terra incognita in QCD and can only be studied in high-energy collisions.

The advantage of using nuclei to explore this regime is the enhancement of the saturation phenomena with increasing  $A$ , making it easier to observe and study experimentally. This dependence is justified by any probe interacting over the distance  $L \sim (2m_N x)^{-1}$  being unable to distinguish between nucleons in the front or back of the Lorentz contracted nuclei once  $L > 2 RA \sim A^{1/3}$ ; the probe then interacts *coherently* with all nucleons. These considerations suggest that  $Q_s^2 \propto (A/x)^{1/3}$ . DIS with large nuclei probes the same universal physics as seen in DIS with protons at  $x$ 's at least two orders of magnitude lower (or equivalently an order of magnitude larger  $\sqrt{s}$ ). When  $Q^2 \gg Q_s^2$ , one is in the well understood “linear” regime of QCD, while we have little theoretical control over the non-perturbative regime at  $Q^2 \lesssim \Lambda_{QCD}^2$ . For large nuclei, there is a significant regime at small  $x$  where  $Q_s^2 \gg Q^2 \gg \Lambda_{QCD}^2$ . This is identified as the saturation regime of strong non-linear gluon fields.

Quite generically, multi-parton correlations are more sensitive to the detailed dynamics of the probed objects than single parton distributions. One of the most captivating measurements in  $e+A$  is that of the azimuthal correlations between two hadrons  $h_1$  and  $h_2$  in  $e+A \rightarrow e' + h_1 + h_2 + X$  processes. These correlations are not only sensitive to the transverse momentum dependence of the gluon distribution, but also to that of gluon correlations for which CGC computations are now available. The precise measurements of these di-hadron correlations at EIC would allow one to extract the spatial multi-gluon correlations and study their non-linear evolution.

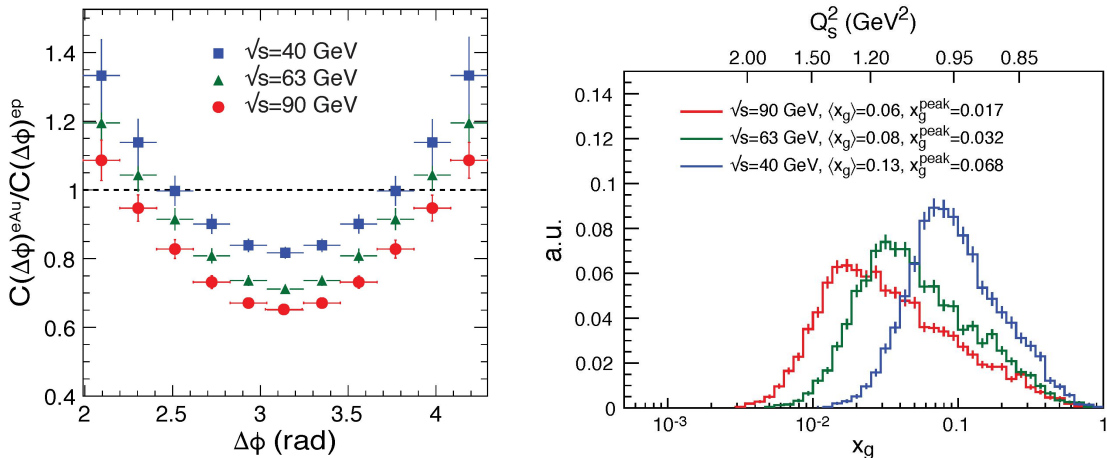


**Figure 9:** *Left:* Ratio of the dihadron correlation functions in  $e+Au$  collisions over those in  $e+p$  for the three center-of-mass energies. *Right:*  $x_g$  distributions probed by the correlated hadron pairs for different center-of-mass energies,  $\sqrt{s} = 40, 63$ , and  $90$  GeV in  $e+Au$  collisions. The average and peak values for the distributions are shown. The gluon saturation scales  $Q_s^2$  corresponding to  $x_g$  values are displayed on top of the plot.

Experimentally, di-hadron correlations are relatively simple to study at EIC. They are usually measured in the plane transverse to the beam axis and are plotted as a function of the azimuthal angle  $\Delta\phi$  between the momenta of the produced hadrons in that plane. Back-to-back correlations are manifested by a peak at  $\Delta\phi = \pi$ . Saturation effects in this channel correspond to a progressive disappearance of the back-to-back correlations of hadrons with increasing atomic number  $A$ . In the conventional linear QCD picture, one expects from momentum conservation that the back-to-back peak will persist as one

goes from  $e+p$  to  $e+A$ . In the saturation framework, due to multiple re-scatterings and multiple gluon emissions, the large transverse momentum of one hadron is balanced by the momenta of several other hadrons, effectively washing out the correlation [16]. A comparison of the heights and widths of the di-hadron azimuthal distributions in  $e+A$  and  $e+p$  collisions respectively would clearly mark out experimentally such an effect. An analogous phenomenon has already been observed at RHIC for di-hadrons produced at forward rapidity in comparing central  $d+Au$  with  $p+p$  collisions at RHIC [17]. In that case, di-hadron production originates from valence quarks in the deuteron scattering on small- $x$  gluons in the target Au nucleons.

To better illustrate the energy dependence, the ratio of the correlation functions in  $e+Au$  over those in  $e+p$  is shown in Figure 9 (left) for three center-of-mass energies. Note the suppression is a factor of 2 at  $\sqrt{s} = 90$  GeV. Measuring a suppression greater than 20% relative to  $e+p$  will be crucial in the comparison of data with saturation model calculations that typically carry uncertainties of at least in this order [18]. The ability to study dihadron suppression over a wide range of  $x_g$  is of the utmost importance for this observable. Figure 9 (right) shows the corresponding  $x_g$  distributions for dihadrons produced at the three different center-of-mass energies. The corresponding  $Q_s^2$  values are provided at the top of the plot. Only a sufficiently wide lever arm will allow one to study the non-linear evolution in  $x_g$  and  $Q^2$  and extract the saturation scale with high precision.

### Machine Requirements for Physics with Nuclei:

The measurement of nuclear PDFs and observables to establish saturation need both nuclear beams with the highest nuclear mass and center of mass energy to reach into a regime to study the onset of saturation and the evolution of its effects with  $x$  and  $Q_s^2$  to reach lowest  $x$  at highest  $Q_s^2$ .

#### 2.1.6 Summary and Conclusions

The EIC will explore how nuclear matter at its most fundamental level is made. The facility will allow to precisely image the quarks and gluons and their interactions and to explore the new QCD frontier of strong color fields in nuclei. The science program described in this overview and in detail in [1,2,19] addresses directly and with high precision the following questions that relate to our fundamental understanding of QCD:

- How are the sea quarks and gluons, and their spins, distributed in space and momentum inside the nucleon? How do the nucleon properties emerge from them and their interactions?
- How do color-charged quarks and gluons, and colorless jets, interact with a nuclear medium?  
How do the confined hadronic states emerge from these quarks and gluons?  
How do the quark-gluon interactions create nuclear binding?
- How does a dense nuclear environment affect the quarks and gluons, their correlations, and their interactions? What happens to the gluon density in nuclei?  
Does it saturate at high energy, giving rise to a gluonic matter with universal properties in all nuclei, even the proton

The parameters for an EIC can be derived from the above questions and have been used to guide the eRHIC and JLEIC pre-conceptual designs being discussed in the following sections:

Contrary to hadron-hadron collisions, **deep inelastic scattering** of electrons off hadrons is a process that allows to the study the inner structure of nuclear matter with unmatched precision. A **high-energy** (20 -- 100 GeV, upgradable to 140 GeV) electron-ion collider is needed to reach from the many-body regime dominated by quark-gluon dynamics to the collective and saturation regimes dominated by gluon effects.

A **versatile range of** electron and ion **beam energies** is required for full coverage of the many-body, collective, and saturation regimes as well as for a broad coverage in  $Q^2$  for studying QCD evolution, disentangling the non-perturbative and perturbative regimes of QCD, and make connection to the kinematic regimes with existing experiments.

**Longitudinal polarized lepton and longitudinal and transversely polarized hadron beams** are required to investigate how the different partons make up the spin of the nucleon and to map the 3-dimensional structure of nuclear matter.

A **versatile range of ion species** is required to study nuclear dependence and saturation effects. A wide range of ion beams from light to heaviest mass offers, e.g., a precise dial in the study of propagation-length for color charges in nuclear matter. Ion beams with heaviest mass are required to possibly identify the saturation regime.

**High luminosity** ( $10^{33-34} \text{ cm}^{-2}\text{s}^{-1}$ ) is required for high precision measurements in various configurations (beam, polarization, ion species), in particular to unravel the multidimensional dependencies of the different physics processes on the kinematic variables ( $x$ ,  $Q^2$ ,  $\Phi_S$ ,  $p_T$ ,  $z$ , and  $\Phi$ ).

### 2.1.7 References

- [1] A. Aprahamian et al., “Reaching for the horizon: The 2015 Long Range Plan for Nuclear Science”, INSPIRE-1398831 [https://science.energy.gov/~/media/np/nsac/pdf/2015LRP/2015\\_LRPNS\\_091815.pdf](https://science.energy.gov/~/media/np/nsac/pdf/2015LRP/2015_LRPNS_091815.pdf)
- [2] The National Academy of Sciences Report, <https://www.nap.edu/catalog/25171/an-assessment-of-us-based-electron-ion-collider-science>
- [3] J. J. Aubert et al., Phys. Lett. B123, 275 (1983). J. Ashman et al., Nucl. Phys. B328, 1 (1989).
- [4] E. Iancu, A. Leonidov, and L. D. McLerran, Phys. Lett. B510, 133 (2001).
- [5] H. Weigert, Prog. Part. Nucl. Phys., 55:461–565, 2005, hep-ph/0501087.
- [6] D. de Florian, R. Sassot, M. Stratmann, and W. Vogelsang, Phys. Rev. Lett. 101, 072001 (2008).  
D. de Florian, R. Sassot, M. Stratmann, and W. Vogelsang, Phys. Rev. D 80, 034030 (2009).
- [7] D. de Florian, R. Sassot, M. Stratmann, and W. Vogelsang, Phys. Rev. Lett. 113, 012001 (2014).
- [8] The 3-D Structure of the Nucleon, M. Anselmino, et al. Eur. Phys. J. A (2016) 52, 164.
- [9] E.C. Aschenauer, S. Fazio, K. Kumericki, and D. Mueller, JHEP09(2013)093.

- [10] K. J. Eskola, P. Paakkinen, H. Paukkunen, and C. A. Salgado, Eur. Phys. J. C77 , 163 (2017).
- [11] E. C. Aschenauer et al. , Phys. Rev. D 96, 114005 (2017).
- [12] M. Froissart, Phys. Rev. 123, 1053 (1961).
- [13] L. V. Gribov, E. M. Levin, and M. G. Ryskin, Phys. Rept. 100, 1 (1983).
- [14] E. Iancu, K. Itakura, and L. McLerran, Nucl. Phys. A708, 327 (2002).
- [15] A. H. Mueller and D. N. Triantafyllopoulos, Nucl. Phys. B640, 331 (2002).
- [16] D. Kharzeev, E. Levin, and L. McLerran, Nucl. Phys. A748, 627 (2005).
- [17] A. Adare et al. [PHENIX Collaboration], Phys. Rev. Lett. 107, 172301 (2011).
- [18] L. Zheng, E.C. Aschenauer, J. H. Lee, and B.-W. Xiao, Phys. Rev. D89 , 074037 (2014).
- [19] A. Accardi et al., Electron Ion Collider: The Next QCD Frontier, Eur. Phys. J. A52, 2016.

## 2.2 eRHIC

Christoph Montag and Vadim Ptitsyn

(for the eRHIC study group)

Mail to: [montag@bnl.gov](mailto:montag@bnl.gov)

Brookhaven National Laboratory, Upton, NY 11973, USA

### 2.2.1 Introduction

Brookhaven National Laboratory (BNL) is proposing eRHIC as a cost-effective implementation of the EIC which meets all the requirements on the accelerator formulated in the White Paper. The EIC eRHIC takes advantage of the entire existing Relativistic Heavy Ion Collider (RHIC) facility with only a few modifications, with only modest cost implications. The well-established beam parameters of the present RHIC facility are close to what is required for the highest performance of eRHIC. The addition of an electron storage ring inside the present RHIC tunnel will provide polarized electron beams for collisions with the polarized protons or heavy ions of RHIC.

The eRHIC design must satisfy the requirements of the science program, while having acceptable technical risk, reasonable cost, and a clear path to achieving design performance after a short period of initial operating time. The strategy for arriving at an optimum design that meets these requirements led to an eRHIC design based on an electron storage ring, referred to as Ring-Ring (R-R) design.

The storage ring based design meets or even exceeds the requirements referenced in the Long Range Plan including the upgraded energy reach:

Center-of-mass energy ( $E_{CM}$ ) of 29 to 140 GeV. The upper limit can only be extended by a significant additional investment in RF equipment; the lower limit is softer and is given by the ability to detect low energy deep inelastic scattered electrons; there is no hard restriction from the accelerator other than reduction in luminosity. The long range plan requires approx. 20 to 100 GeV;

- A luminosity of up to  $10^{34} \text{cm}^{-2} \text{sec}^{-1}$  ; the long range plan requires  $10^{33}$  to  $10^{34} \text{cm}^{-2} \text{sec}^{-1}$ ;